Available online at www.sciencedirect.com

SciVerse ScienceDirect

Solar Energy 86 (2012) 208–219

SOLAR ENERGY

www.elsevier.com/locate/solener

Experimental study of small-scale solar wall integrating phase change material

Laurent Zalewski [a,b,*], Annabelle Joulin [a,b], Stéphane Lassue [a,b], Yvan Dutil [c], Daniel Rousse [c]

[a] Univ Lille Nord de France, France
[b] UArtois, LGCgE, F-62400 Béthune, France
[c] T3E Industrial Research Chair, Ecole de technologie supérieure, 1100, rue Notre-Dame, Montreal, QC, Canada H3C 1K3

Received 7 December 2010; received in revised form 9 September 2011; accepted 22 September 2011
Available online 29 October 2011

Communicated by: Associate Editor Halime Paksoy

Abstract

Solar walls have been studied for decades as a way of heating building from a renewable energy source. A key ingredient of these wall is their storage capacity. However, this increases their weight and volume, which limits theirs integration into existing building. To aleviate this problem, storage mass is replaced by a phase change materials. These allow to store a large amount of energy in a small volume, which brings the possibility of retrofit trough use of light prefabricated module.

This article presents an experimental study of a small-scale Trombe composite solar wall. In this case, the phase change material was inserted into the wall in the form of a brick-shaped package. While this material can store more heat than the same volume of concrete (for the same temperature range), it shows a very different thermal behavior under dynamic conditions. A particular attention is focused on the delay between the absorption of solar radiation and the energy supplied to the room. The energy performance of the wall from heat flux measurements and enthalpy balances are also presented.

Keywords: Solar wall; Phase change material; Energy storage; Latent heat

1. Introduction

Given the predictable rise in the cost of fossil fuels and the desire to reduce carbon emissions, many countries have enforced policies to improve energy efficiency, while reducing the fossil fuel usage. The building sector is a key to the success of such policies. Building consumption in the EU was 37% of final energy in 2004, (around 41% of total US energy use in 2002). One way to reduce these numbers is to increase the insulation requirements of building envelopes through the formulation of ever more demanding regulations. However, there are some practical, physical, and financial limits to this approach. One way to overcome these limitations is to transform the role of the envelope from a passive barrier to heat loss into an active heat recovery system. From this point of view, it is important to propose schemes to reduce losses and increase building solar gains while maintaining occupant comfort in all seasons (Gratia and Deherdea, 2007; Alzoubi and Alshboul, 2010; Ahmad et al., 2006; Diaconu and Cruceru, 2010).

In this context, our laboratory has been working for several years on the characterization and optimization of Trombe walls (Shen et al., 2007; Zalewski et al., 1997, 2002). In the study presented here, the concrete storage wall is replaced by a wall into which elements containing hydrated salts are integrated. The objective of this research is to characterize the storage capability and the dynamical behavior of this wall under actual weather conditions.

* Corresponding author. Address: UArtois, FSA, Technoparc Futura, 62400 Béthune, France. Tel.: +33 321 637 153.
E-mail address: laurent.zalewski@univ-artois.fr (L. Zalewski).

0038-092X/$ - see front matter © 2011 Elsevier Ltd. All rights reserved.
doi:10.1016/j.solener.2011.09.026

Nomenclature

P	power (W)
R	cross-correlation function
S	area (m^2)
t	time (s)
T	temperature (°C)
V	velocity ($m\ s^{-1}$)

Greek letters:

ρ	density ($kg\ m^{-3}$)
φ	heat flux (W/m^2)
τ	time lag (s)

Subscripts/superscripts:

air	air
exc	exchange area
enth	enthalpic method
ext	exterior (exterior face)
fluxm	fluxmetric method
int	interior (interior face)
lv	lower vent
solar	solar radiation
uv	upper vent
PCM	phase change material

These parameters being both qualitatively and quantitatively different than sensible heat storage material (ex: concrete) normally used in such wall. This knowledge is essential to optimization of the performance of this peculiar type of Trombe wall.

2. The composite solar wall

The composite solar wall (Zrikem and Bilgen, 1987, 1989) (Fig. 1) is formed from outside to inside of several layers: a semi-transparent cover, a closed cavity, a storage wall, a ventilated air cavity and an insulating panel where two vents allow the warm air to enter inside the room. The recovery unit works as follows: The transparent layer transmits the highest possible portion of the incident solar beam, the storage wall receives and absorbs a part of the transmitted solar energy and heats up. This wall remits in a lower wavelength and radiation is trapped by greenhouse effect in the closed cavity, some losses occur due to natural convection in the closed cavity. The storage wall stores and transmits the remaining part of the absorbed energy to the building. This energy is transferred to the room to be heated by natural convection occurring in the ventilated channel. A very small part of the energy is also transmitted by conduction trough the wall into the room. The warm air supply can be suppressed thanks to the control of the air circulation, thereby avoiding overheating in mid-season or summer. These free solar gains have to be distinguished from direct solar gains. A typical solar wall stores heat during sunny periods and releases it after a delay depending on its geometric and thermophysical characteristics. The heat recovery occurs out of phase compared to the direct solar gain and thus reduces the risk of overheating.

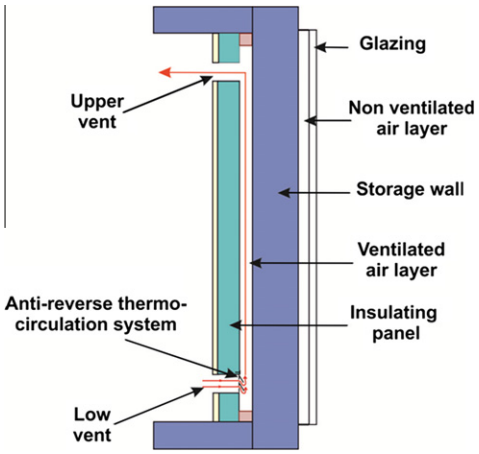

Fig. 1. Composite Trombe wall.

The composite solar wall provides several advantages. Heating is controllable at any time by acting on the air flow into the ventilated channel. Its thermal resistance is high due to the presence of the wall insulation and the ventilated channel. The infiltration of fresh air through the outer cover is negligible. Due to its high thermal resistance and the possibility of controlling the air flow, the heat loads are limited during summer. In addition, these can be minimized further by placing a curtain or a shutter in front of the glazing.

The main disadvantage of this type of walls or any types of Trombe walls resides in the need for a mechanism to prevent the reverse thermocirculation. This phenomenon occurs when the storage wall becomes colder than the ambient air of the room. The air could then be cooled and sent back into the room through the lower vent. However, a simple mechanism using a plastic film placed in the lower vent can eliminate this problem. When the air is heated by the wall, a slight depression due to natural convection removes the film from the vent. On the other hand, the plastic film is pressed against the vent preventing any reverse air circulation inside the channel. The behavior allows the mechanism to act effectively like a thermal diode (Zalewski et al., 1997).

The first wave of studies on the utilization of phase change material in a Trombe wall occurred around 1980.

Askew (1978) used a collector panel made of a thin slab of paraffin placed behind the double glazing of a building and found that thermal efficiency were comparable to a conventional flat plate collector. Telkes (1978, 1980) worked on a Trombe wall using Glaubert salt behind a polyhedral glazing. Her work was only a first order theoretical analysis demonstrating the potential of this approach to reduce mass and volume involved. Solomon (1978), using computer simulation, derived qualitative conclusion about how best to choose the PCM for energy storage in a wall. Farouk and Guceri (1981) created a one dimensional numerical model of a Trombe wall using PCM ($Na_2SO_4{\cdot}10H_2O$ and P-116 wax). They demonstrated that it could provide similar results to a masonry wall, while eliminating its undesirable properties. Swet (1980) reviewed the state of the art in the usage of PCM for thermal storage in building and noted that PCMs provide equivalent thermal storage in a much thinner wall.

Bourdeau and Jaffrin (1979) and Bourdeau et al. (1980) modeled and tested a Trombe wall and diode wall using chliarolithe ($CaCl_2{\cdot}6H_2O$) with the addition of diatom powder as a PCM. Numerical model demonstrated that a 3.5 cm wall using PCM could replace a 15 cm wall of concrete, while the phase delay of the PCM wall was smaller and that the heat transfer was spread over a longer period. Experimental tests were conducted on two tests cells where the storage wall had 5 cm PVC tubes embedded. Those tubes were filled with either water or chliarolithe. This wall was placed behind a single glazing. The wall using latent heat was able to capture about twice the heat of the one with water. To minimize thermal loss trough the glazing, a diode wall was designed. Such wall use a solar collector separated from the storage volume by an air channel. In daytime, a forced convection transports the heat from the collector to the storage volume. Like in a Trombe wall, heat is transmitted to the room by conduction trough the storage volume. Model indicated that this configuration was much more efficient if it used latent heat storage. The first experimental setup used 8 cm PVC tubed embedded in a plaster wall. A second configuration used hollow concrete bloc where part of the void was used to carried the heat, the other part been filled with PCM. In both configuration, the heat was effectively stored through the day and released in a uniform way.

In a parallel work, Bourdeau (1980, 1982) studied the behavior of Trombe wall made of polyethylene container place on a wood shelve behind a double glazing. Tests were carried at Los Alamos laboratory (DOE 1980, Los Alamos 1980). These demonstrated that latent heat storage can become saturated after a few days of operation. These experimental results were used to validate the numerical model, which demonstrated that a Trombe wall with latent heat storage was more efficient than a concrete one. Optimum thickness of a latent wall was a factor 4 smaller than one in concrete, which translate in a factor 6 in mass. Also, an optimal melting temperature, which is a function of the climate, the heating load and the heat transfer coefficient between the wall and the room could be derived from the model.

Benard et al. (1982) studied experimentally a paraffin Trombe wall with a double glazing. They noted that the thermal efficiency of the wall itself showed little sensitivity to the presence of thermocirculation. Nevertheless, they pointed out that forced circulation would improve the performance be reducing the overheating and the convective loss to the outside at the beginning of the night be moving the heat into the room. Benard et al. (1985) carried out a 3 years experiment on Trombe walls (40 cm concrete, 8 cm hard paraffin and 8 cm soft paraffin). In addition to the normal weather conditions, their tests cells allowed the exploration of various degree of coupling between the wall and the room behind. They also noted that the lower weight of the latent heat storage wall (one-twelfth smaller) compare to concrete was much better suited for a retrofit.

Knowles (1983) presented numerical results as well as approximate simple stationary state formula with the purpose of establishing guidelines for the design of low-mass, high-efficiency walls. One conclusion was that thermal resistance of the wall should be as low as possible. Exploration of binary and ternary composite of metals, masonry and phase change materials was studied. Compared with concrete, paraffin–metal mixtures were found to offer a 90% reduction in storage mass and a 20% increase in efficiency.

Christensen (1983) did a parametric analysis that allowed the identification of factors limiting performances of Trombe wall and presented configuration for enhanced PCM performance. Benson et al. (1985) carried an analysis on PCM (polyalcohols) properties that prefigures contemporary studies. They also did a computer simulation on the performance of PCM inclusion in a Trombe wall and compared them to a concrete wall. The optimum melting temperature was found to be 27 °C for this wall. An increase in thermal diffusivity was shown to be beneficial to the performances. Accordingly laboratory tests demonstrated that diffusivity could by increase by a factor five by the addition of 2% of graphite, which should lead to a 30% gain in performance. They concluded that a Trombe wall with PCM could be a factor four thinner and a factor nine lighter than its equivalent in concrete. However, its cost would be more expensive by a factor 2. Wild et al. (1985) measured the performance of PCM encapsulated in rigid plastic panel in calibrated hot box. The accurate measurements of heat flux during the discharge cycle of Trombe wall systems containing the PCM panels were obtained.

Tiwari et al. (1988) created a numerical model of a composite wall composed of one layer of PCM material and one layer of water to transfer heat from a sunspace to an adjacent room. This combination combined the high storage capacity of the PCM and the high heat transfer coefficient of water. Ghoneim et al. (1991) did a numerical analysis and simulation of a Trombe Wall with different thermal storage mediums: sodium sulfate decahydrate,

medicinal paraffin, P116-wax, and traditional concrete. Their simulation results showed that PCMs have much better thermal storage performance than the traditional concrete and among the phase change material Glauber's salt ($Na_2SO_4 \cdot 10H_2O$) presented the best properties. They noted that a lower melting temperature (20–30 °C) improved the overall efficiency of the system and that the grade of the paraffin had little impact on the system performances.

Stritih and Novak (1996) studied numerically and experimentally a wall composed of a transparent insulation material covering a solar collector made of black paraffin. An air channel behind the solar collector brought the preheated air for the ventilation of the house. Their numerical analysis indicated that the optimum thickness was 50 mm and the melting point a few degrees above room temperature. Manz et al. (1997) studied a wall system composed of transparent insulation material and translucent phase change material used both for solar heat storage and daylighting. The PCM was hexahydrated calcium chloride ($CaCl_2 \cdot 6H_2O$) with 5% of additive. Their numerical model included the radiative heat transfer in their dynamical model of the PCM. Experimental data were gathered over a period of 5 month. Authors concluded that performance would be improved by the reduction of melting temperature from 26.5 to 21 °C.

Onishi et al. (2001) studied the thermal behavior of a room with a Trombe wall using computational fluid dynamics. In addition to solar energy, supplement electric heating was embedded into the wall. Seven configurations of were studied (concrete slab, three different PCM slabs with and without electrical heater. Simulation results indicated that this approach is worthwhile for low energy house applications. Nevertheless, subsequent optimization work was needed on the PCM melting temperature and the size of the wall. Eiamworawutthikul et al. (2002) noted the lack of universal recommendation as how the PCMs should be incorporated in a building design. They also carried a preliminary numerical study on a concrete Trombe wall impregnated 20% by weight of paraffin. Their analysis demonstrated a threefold reduction in the wall thickness compare to a standard concrete wall.

Khalifa and Abbas (2009) created a dynamic simulation computer model of a south-facing thermal storage wall. Two types of PCMs were examined, the hydrated salt $CaCl_2 \cdot 6H_2O$ and paraffin wax encapsulated in copper capsules with length to diameter ratio of 0.76. They found that a storage wall 8 cm thick made from the hydrated salt maintained the temperature better than a 20 cm thick concrete wall and the 5 cm thick wall made from paraffin wax.

3. The investigated solar wall

The solar wall studied in this paper is a small-scale wall (see Figs. 2 and 3). It is surrounded by insulated walls consist of an insulation (5 cm) and wood (13 mm). The opposite side of the solar wall is open to the room where the set-up is installed. The storage wall incorporates

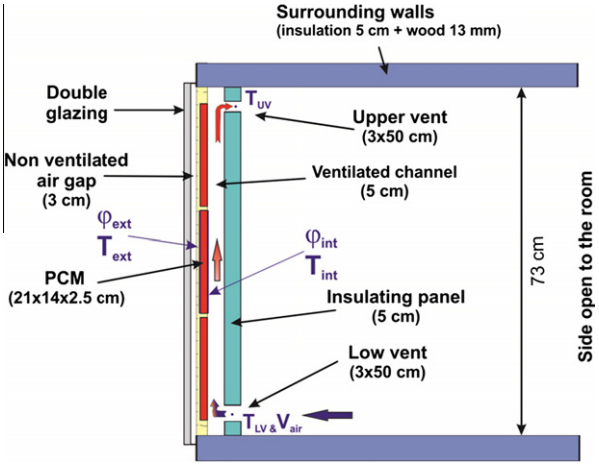

Fig. 2. Vertical section.

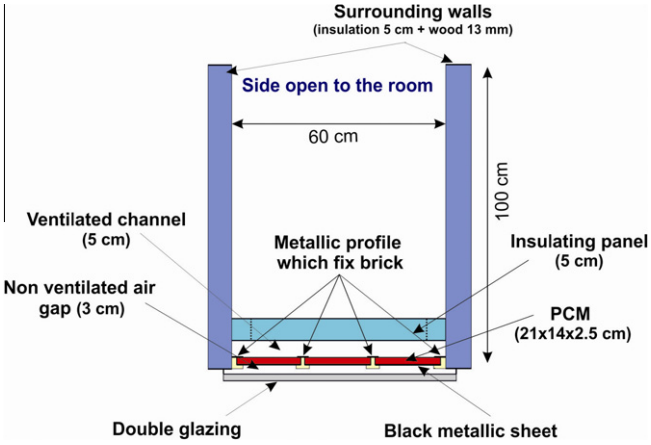

Fig. 3. Horizontal section.

Fig. 4. PCM brick.

rectangular bricks containing a phase change material. The PCM is packed in a polyolefin envelope in a brick shape (21 cm × 14 cm × 2.5 cm) (see Fig. 4). The PCM

used is a mixture of hydrated salts [water + calcium chloride ($CaCl_2$) + potassium chlorides (KCl) + additives] provided by the company Cristopia (Zalba et al., 2003; Cristopia website), its melting point being 27 °C. Thermophysical properties (heat capacities, thermal conductivities of solid and liquid phases and latent heat) of this material were determined under the conditions of use and including the envelope (Younsi et al., 2007, 2008). The wall itself is composed of nine bricks arranged in 3 × 3 array and supported by a wooden frame. This leads to an exchange area of 60 cm × 73 cm. On its external face, the frame is used to maintain black-coated metal plates used as an absorber plate (Fig. 5). No anti-reverse circulation system has been installed in this set-up.

The instrumentation consists of a pyranometer, thermocouples, tangential gradient fluxmeters (Leclercq and Thery, 1983), and one anemometer. The pyranometer is located in the vertical plane of the facade receiving the incident solar flux. Two fluxmeters and two thermocouples (φ_{ext}, T_{ext}, φ_{int} and T_{int}), installed on the two largest surfaces of the central brick, measure the thermal fluxes (Fig. 2). Sandwiched between the absorber and the bricks, the fluxmeter φ_{ext} measures the incoming and outgoing heat flux (solar radiation and exchanges between the brick and the double glazing). On the ventilated channel side, the fluxmeter φ_{int} measures the convective and the radiative heat exchanges between the bricks and the facing insulated wall (Fig. 2). The thickness of the fluxmeters is 0.2 mm, and their sensitivity about 120 μV W^{-1} m^2 for a sensor having an active surface of 14 × 21 cm^2. The calibration device makes it possible to calibrate these sensors with a precision of about ±3%.

Two other thermocouples measure the air temperature at the lower vent (T_{lv}) and at the upper vent (T_{uv}) while the anemometer measures the inlet air velocity (V_{air}). The thermocouples are T type with a diameter of 0.1 mm. The thermocouples were calibrated in a temperature calibrator (CS172 Eurolec), the uncertainty on thermocouple temperature measurements is estimated at ±0.5 °C.

The measurement of the air velocity is done at the lower vent. Choice of the position of the anemometer at the lower vent is based on the fact that there are strong temperature gradients and velocity outputs into the channel and at the exit while in the lower part, the air temperature is homogeneous and velocity profile is much more uniform. The average velocity is estimated using the Log-Linear method (ASHRAE, 1993) providing sufficiently high accuracy (±3%) in flow integration. The recommended procedure indicates that any rectangular duct dimensions require a minimum of 25 velocity measurements. The measuring points are distributed on a 5 × 5 grid as shown in Fig. 6.

The ratio of the two values (velocity at the center of vents and the average velocity) determines $Coef_{Lv}$. The coefficient, $Coef_{Lv}$, is then related to the average velocity in the cross-section. It is based on a measuring point at the center of vent, combined with the average velocity measurements. We must also verify that the temperature measurement (T_{uv}) is representative of the average temperature of the air output.

4. Results

4.1. Heat fluxes and temperature

For this study, 2 weeks from April 22 to May 5 2008 were chosen. In northern France (Bethune: 50.51°N 2.65°E), this period corresponds to the spring: the solar gains are significant but the outside temperature remains cool. Fig. 7 shows the variation of the incident solar radiative flux impinging on the solar wall (φ_{solar}) and the heat flux (φ_{ext}) measured on the outer side of the brick in contact with the absorber with respect to time.

Fig. 5. Photo of the exterior face of the storage wall.

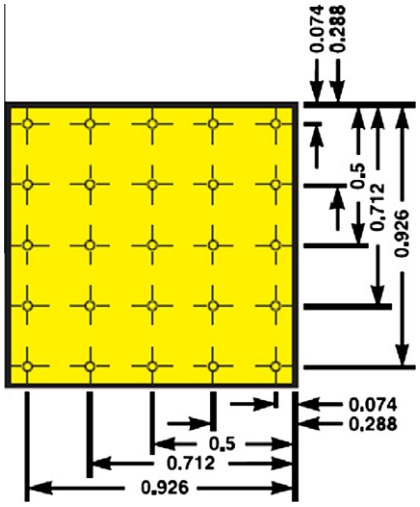

Fig. 6. 25 points log linear-traverse for rectangular ducts.

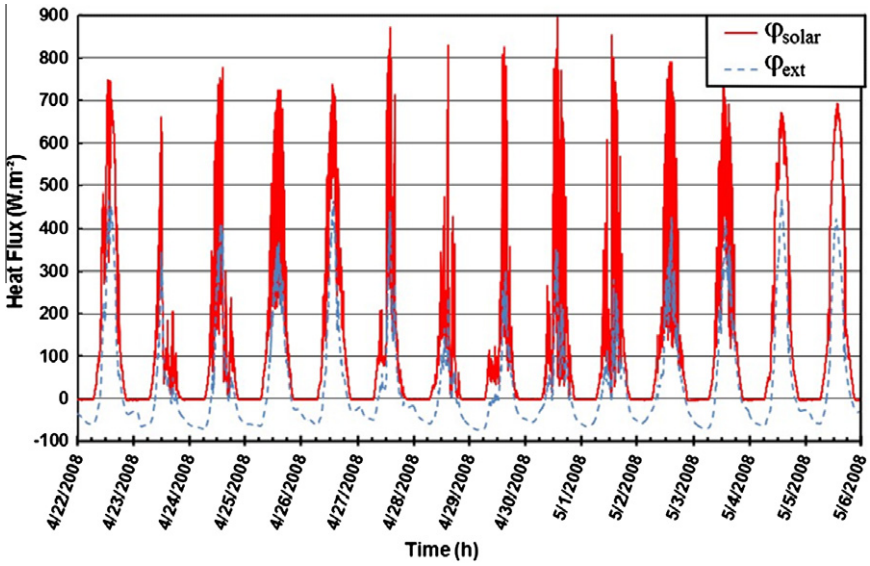

Fig. 7. Incident solar radiative flux (φ_{sol}) and heat flux absorbed by the brick (φ_{ext}) as a function of time for a period of 14 days in April–May, 2008.

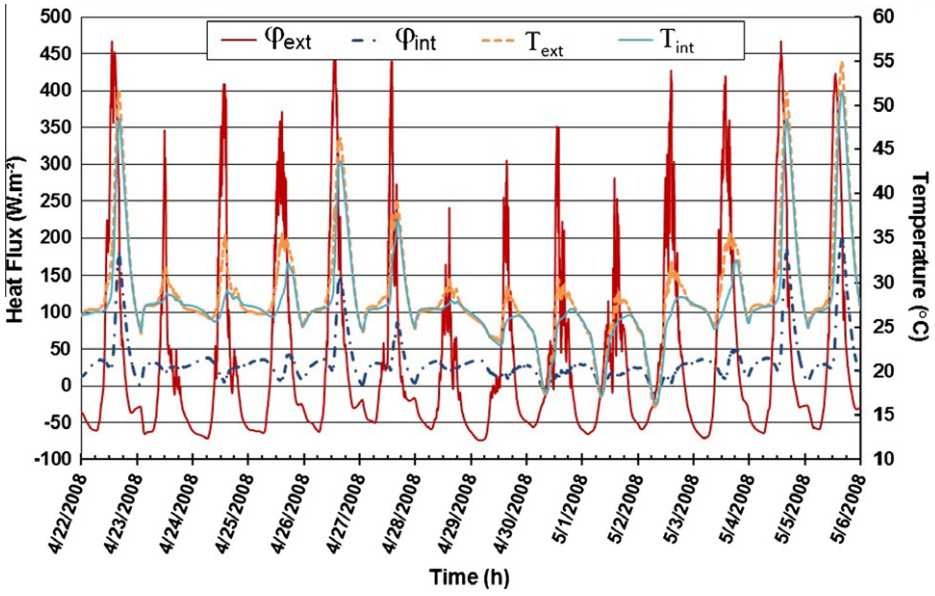

Fig. 8. Heat fluxes φ_{ext}, φ_{int} and temperatures T_{ext}, T_{int} measured on both sides of the PCM brick as a function of time for a period of 14 days in April–May, 2008.

Fig. 8 shows the evolution of the heat flux and the temperatures measured on both sides of the brick during the same period.

These two figures show that the brick can absorb a large quantity of heat when the solar radiation is the most intense (800–900 W/m^2 for the solar flux and 450 W/m^2 for the flux entering the PCM brick). The heat flux φ_{ext} becomes negative at sunset and some of the energy, stored during the day, is exchanged with the external environment (through the double glazing). On the other side of bricks, the internal flux φ_{int} is almost always positive within the studied timeframe and generally varying between 0 and 50 W/m^2. The temperature of the brick reached 55 °C on its outer surface and 52 °C on its inner surface on the last day of the test.

Fig. 9 shows the temperatures measured in the ventilated channel at the lower and the upper vents. This difference increases when increasing solar flux. Free convection is dominant since air velocities are lower than 25 cm s^{-1}.

From these data, we will further analyze the efficiency and the thermal behavior of the wall containing phase change material.

4.2. Dephasing

In a previous work (Zalewski et al., 1997), the delay between the solar irradiation and the internal heat flux has been studied when the composite solar wall was

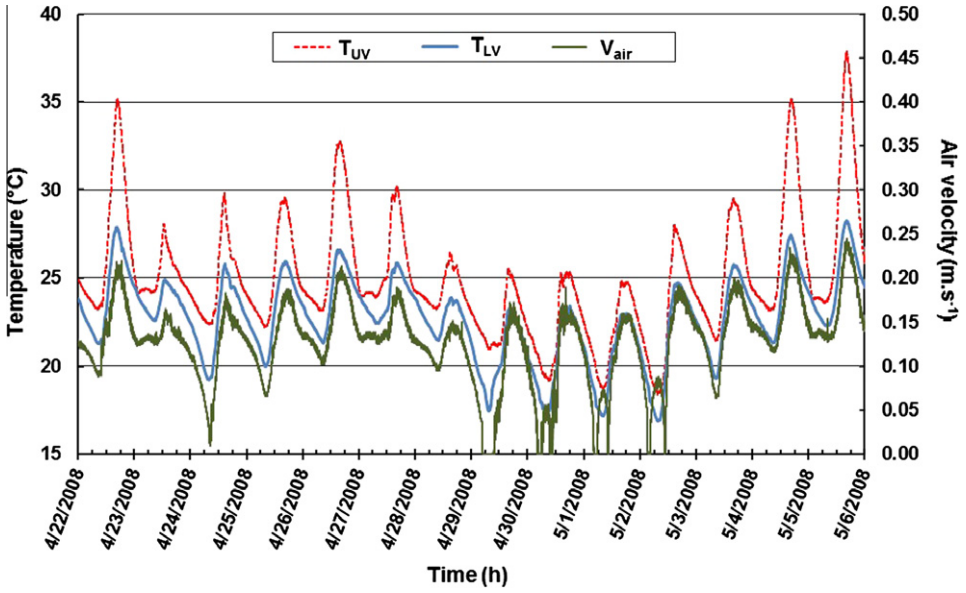

Fig. 9. Temperatures at the level of the upper and lower vents and air velocity at the lower vent in the channel as a function of time for a period of 14 days in April–May, 2008.

composed of a concrete 15 cm thick slab. This specific setup the delay has been estimated at 5 h 55 min.

Like in our previous, we used the cross-correlation to estimate the delay (Takamoto et al., 2001; Şişbot, 2005). To estimate the delay between absorbed flux, (φ_{ext}), and transmitted flux, (φ_{int}), it is convenient to use the cross-correlation function. Since, φ_{ext} and φ_{int} are two independent variables, the cross-correlation function between these two quantities is expressed as:

$$R_{\varphi_{ext},\varphi_{int}}(\tau) = \int_{-\infty}^{+\infty} \varphi_{ext}(t).\varphi_{int}(t-\tau)\cdot dt \quad (1)$$

This function has the following properties:

- $R_{\varphi_{ext},\varphi_{int}}(-\tau) = R_{\varphi_{ext},\varphi_{int}}(\tau)$.
- When $R_{\varphi_{ext},\varphi_{int}}(\tau) = 0$, the two processes $x(t)$ and $y(t)$ are not correlated.

When two processes are the most correlated, this value τ defines the time delay (dephasing).

Fig. 10 shows the result of the cross-correlation function calculated between the heat fluxes (φ_{ext} and φ_{int}) during 3 weeks.

Fig. 10 indicates that the energy supplied to the 2.5 cm thick brick is restituted to the room with a delay of 2 h 40 that is more than twice shorter than a 15 cm thick concrete wall (Zalewski et al., 1997). Similar behavior was observed experimentally by Bourdeau and Jaffrin (1979) and Bourdeau et al. (1980).

4.3. Efficiency of the solar wall composite

The variations of the values of φ_{solar}, φ_{ext} and φ_{int} with respect to time for four sunny days of the above-mentioned period (Figs. 7–9) are shown in Figs. 11 and 12.

Fig. 11 indicates globally that the maximum incident solar flux on the vertical glass wall reaches 700 W/m^2, the heat flux entering the brick is at the most 400 W/m^2, and the global heat flux flowing into the ventilated channel is at the most 200 W/m^2. After 6:00 pm, energy is released to the outside via the closed cavity: a double glazing could help in reducing these losses. On the other hand, Fig. 11 shows that after 6:00 pm the unit delivers a net heat flux to the ventilated layer until after midnight. Moreover, the time delay for maximum delivery corresponds exactly to a period for which the energy consumption is very high in Europe. Thus, installing such "balanced" units could cut the peak power consumption in the end of the afternoon.

Fig. 12 indicates the high temperatures reached by the brick (50–60 °C) and the maximum exit air temperature which is almost reaching 40 °C. On such a unit, the time delay cannot be perceived clearly as the maxima in temperature occur almost simultaneously on both sides of the brick and at the ventilated layer outlet.

The interesting thing about PCM can be observed in both Figs. 11 and 12 at about 2:00 am: In Fig. 11, solidification of the PCM is shown as the heat recovery (and heat losses to the environment unfortunately) are both increasing. The heat recovery throughout the night is maintained at about 25 W/m^2. In Fig. 12, this induces a temperature rise on both sides of the brick and make the outlet temperature of the air almost constant throughout the night and this although the inlet temperature drops until the morning. All that is due to the amount of heat that the PCM releases when it solidifies.

4.3.1. Energy recovery

Over the period of 24 days (21 April–15 May 2008), including heat losses at night, the accumulation of solar energy irradiating the glass was measured to be equal to

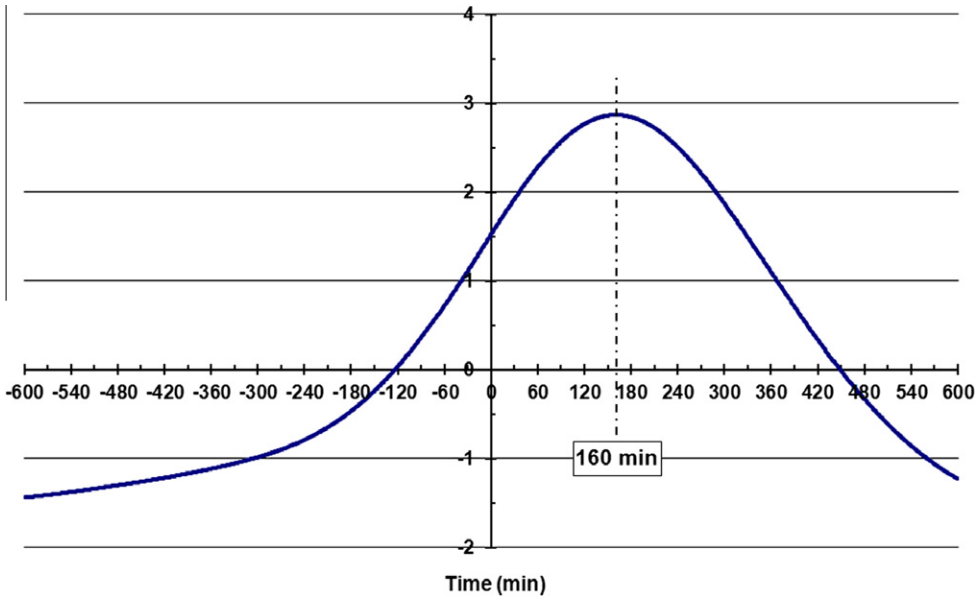

Fig. 10. Calculated cross-correlation function.

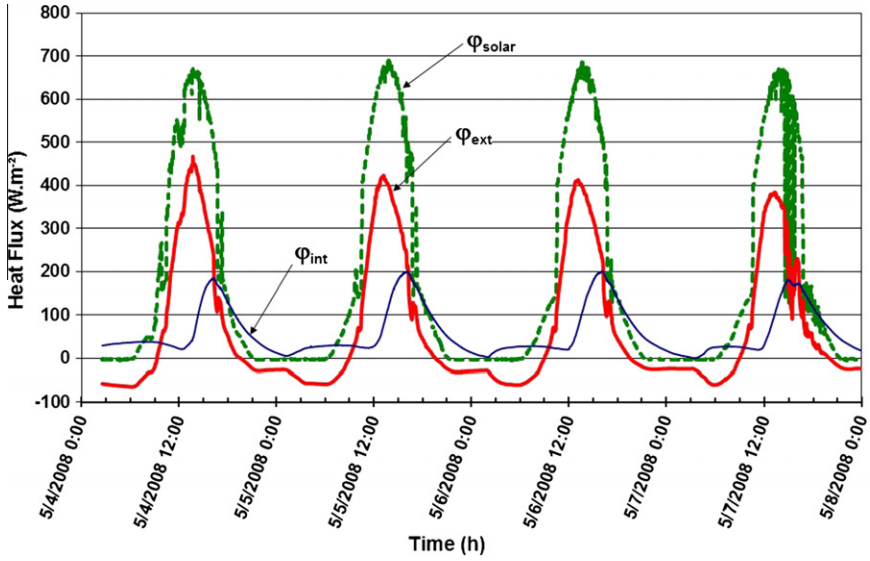

Fig. 11. Heat flux measurements, φ_{sol}, φ_{ext}, and φ_{int} as a function of time for a period of four sunny days in May, 2008.

78 kWh/m^2. Of these, the brick was found to absorb only 37.7 kWh/m^2; 49% of the incident solar energy. The energy released to the channel was measured to be 23.5 kWh/m^2, which is only 68% of the absorbed energy. Overall, the thermal efficiency of the wall is only ≈30%. These percentages show that some optimization is desirable. This could be done, for instance, by replacing the traditional double glazing used in this experiment, by a low emissity double glazing to limit radiative heat losses to the outside (16% energy absorbed in our case).

It would also be desirable to increase heat exchanges within the channel using a fan (Jie et al., 2007; Boutin and Gosselin, 2009). Another solution is to use a PCM having a higher melting temperature (≈40–50 °C) to increase the wall temperature to promote the natural convection. This would increase heat gains due to a higher temperature difference between the temperature of the room and the wall. Another advantage: the probability that the phase change material solidifies completely during the night would be higher than in the present study. However, the losses to the outside would be increased; a comprehensive study using numerical models would be very useful to assess the impact of this change on the efficiency of the solar wall. The model could as well be used to study the energy efficiency of solar walls in different locations and under different climatic conditions.

4.3.2. Energy balance of air channel

It should be noted that in our calculation, the heat transfer is considered per m^2 of wall. In reality, the absorptive

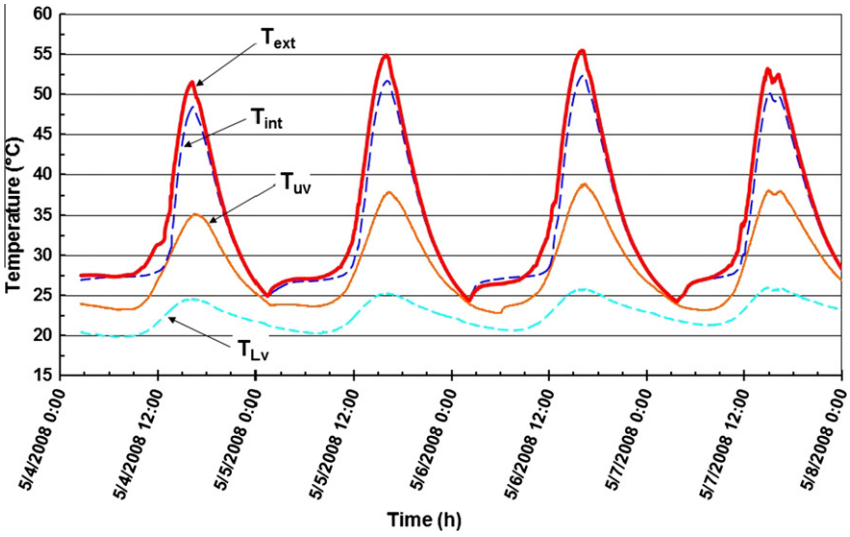

Fig. 12. Measured temperatures.

surface of PCM is not equal to the surface of the glass due to the presence of the framework supporting the brick. The energy balance of the cavity was calculated using two different methods validated in previous studies (Zalewski et al., 1997, 2002). The first method is based on a direct heat flux measurement and the second method is based on the enthalpy balance of air between the channel inlet and outlet. These methods are briefly described below:

4.3.2.1. Flux balance. This method is based on the idea that the whole amount of heat recovered by the air in the ventilated channel is provided by the bricks. In this case, these exchanges are measured by the fluxmeter φ_{int}; this fluxmeter has the same radiative properties as the bricks. To obtain the total heat recovered by the air, it is necessary to multiply this heat flux by the number of bricks, assuming that the central brick is representative of the nine bricks thermal behavior:

$$P_{fluxm} = 9 \cdot \varphi_{int} \cdot S_{exc} \quad [W] \tag{2}$$

with $S_{exc} = 0.14 \times 0.21\ m^2$ (exchange surface brick/air).

4.3.2.2. Enthalpy balance. We consider in this case that the energy exchange between the air and the storage wall is equal to the air enthalpy variation. The heat recovered by the air (P_{enth}) is determined experimentally using the following equation:

$$P_{enth} = Coef_{Lv} \cdot V_{air} \cdot S_{Lv} \cdot \rho_{air} \cdot (T_{uv} - T_{Lv}) \quad [W] \tag{3}$$

The cross section of the lower vent (S_{Lv}) is identical to that of the higher vent (S_{uv}).

The results obtained through the two methods can be compared. To ease the comparison, the same 4 days used previously are analyzed (Fig. 13).

The two methods used to determine the thermal heat recovered show a similar behavior. However, in periods of low heat exchanges, in the early morning or at the end of the discharge period, significant differences between both methods can be observed. The enthalpy balance seems smoother while fluxmeter records presenting more fluctuations. This could be explained by the fact that the heat flux balance is measured from the central brick. Through the phase change, a substantial amount of heat is released and measured by the fluxmeter. It is unlikely that the phase change occurs at the same time for the nine bricks. This explains why the same behavior is not found in the enthalpy balance (except in the middle of the period at 6:00 am). It is also notable that when the heat exchanges are weak, heat fluxes, velocities, and temperature differences between the air vents are reduced. This increases the uncertainty of the heat recovery calculation but otherwise does not significantly affect the total exchanged energy.

If this exchanged energy is accumulated for the 24 days (14 days of this period are represented in Figs. 7–9), the total of recovered energy is estimated at 6.6 kWh for the enthalpy method (P_{enth}) and 6.2 kWh for the heat fluxmeter method (P_{fluxm}). The difference between both methods is about 6%.

4.4. Study of the brick containing the PCM

Several articles of the literature (Sandnes and Rekstad, 2006; Yinping et al., 2007) dealt with supercooling occurring in PCM. With our instrumental set-up, this phenomenon can be detected and investigated. Fig. 14 shows the heat flux and temperatures recorded on both sides of the brick. To help the visualization of the phenomenon, we have plotted two consecutive days taken from the 2 weeks period shown in Figs. 7–9.

Shortly after 1:00 pm (time ① identified in Fig. 14), the heat flux (φ_{ext}) is at its maximum. At this moment, the solar flux is maximum. At time ②, temperatures T_{ext}, T_{int} and heat flux φ_{int} are reaching their maximum value. This

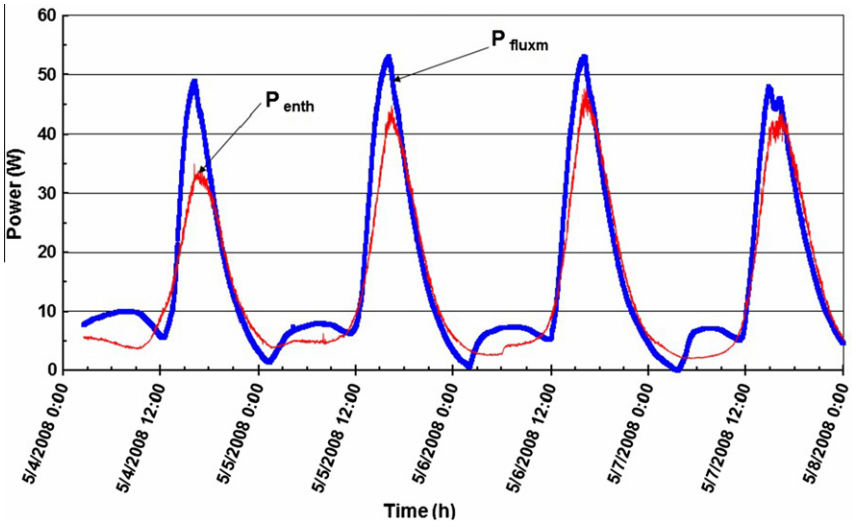

Fig. 13. Enthalpy balance and heat flux balance.

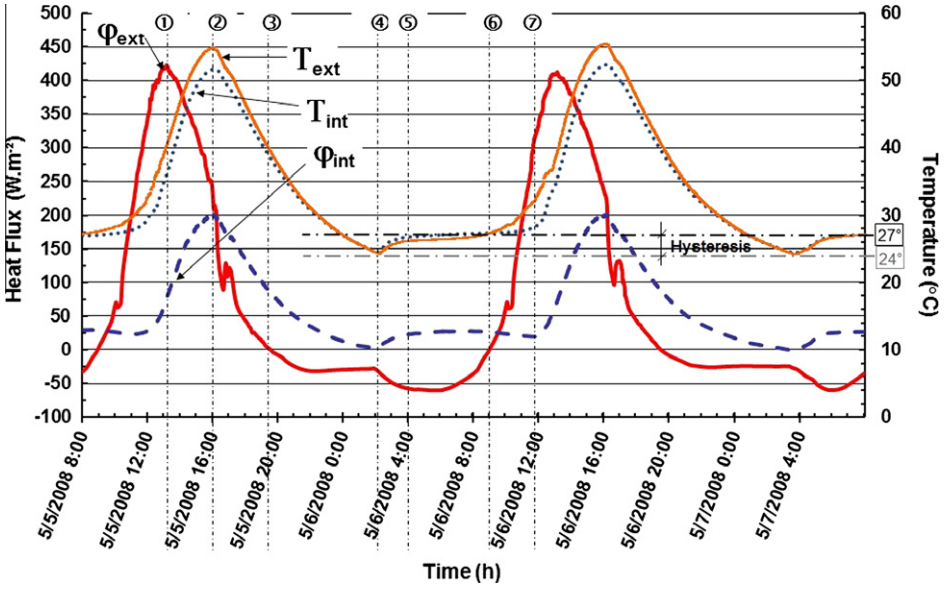

Fig. 14. Flux and temperature measured on both sides of the brick.

occurs at 4:00 pm, less than 3 h after the peak of sunshine (2 h 40 calculated in Section 1.3). Between the instants ① and ②, the intensity of solar radiation has decreased and therefore the heat flux entering the brick also. Despite this decrease, the gains are still positive and the brick continues to store heat; the PCM and its envelope warms up. T_{ext} is naturally higher than T_{int} due to solar heat outside. This is a phase of storing and transferring energy to the inner ventilated cavity. At 4:00 pm, the brick releases, energy by convection and radiation within the ventilated channel. Then, on that same face, between 4:00 pm and 2:00 am, the next day (between ② and ④), the brick releases heat (T_{ext} and T_{int} decreases) and still provides heat to the air ($\varphi_{int} > 0$). However after 7:00 pm (③), the heat flux becomes negative on its outer face ($\varphi_{ext} < 0$); hence the brick yields heat to the closed gap and exterior glazing. Through all these phases, the PCM is in its liquid form.

At 2:00 am (period ④), there is an inflection in the curves. Previously, the two sides of the brick were at the same temperature and then reached 24 °C, the temperatures rise suddenly and the heat flux increases too. This is caused by the solidification of the PCM. While solidifying, the PCM releases the latent heat contained, and as this amount of heat cannot be evacuated instantly from the brick, the temperature within the material increases. Obviously, the heat evacuates more easily from the outside because the flux φ_{ext} increases more than the flux φ_{int}. On the other hand, as the heat flux φ_{int} becomes larger than before the solidification process, exchanges in the channel are revitalized. This is a positive point for the efficiency of the system.

From 4:00 am (⑤), the temperature stabilizes around the melting temperature of the material, i.e. 27 °C. Around 6:00 am, the sun rises and the heat flux φ_{ext} increases and

starts to become positive at 9:00 am (⑥). Between ⑤ and ⑥, the temperatures remain constant about the melting temperature. At 9:00 am (⑥), φ_{ext} is positive and the temperature T_{ext} exceeds the melting temperature and increases steadily. The PCM has melted at the outside face and the melting front moves towards the internal part of the brick. Around midday (⑦), the melting front reaches the inner side, φ_{int} increases significantly, the temperature T_{int} increases too. The whole PCM is melted and the temperature rises as the brick stores sensible heat.

These curves clearly show the storage–discharge phases of the PCM and the temperature of the melting point. They highlight the hysteresis phenomenon between the solidification temperature and the melting point temperature of the material. When the sun rises, φ_{int} is always positive, this means that the bricks have not entirely released the energy accumulated the previous day; the ventilated channel did not permit to extract all the available energy.

5. Conclusions

In this paper, the results of a thermal study on a small-scale solar wall composite incorporating phase change material were presented. These were obtained thanks to the implementation of an experimental set-up facing real weather conditions.

One advantage of the composite solar wall is that the solar gains are released with a time lag. These gains during the evening and at night are added to direct solar gains through windows received during the day. The time lag depends on the nature of the storage wall and its thickness. In a previous work, the study of the time lag of concrete wall storage with a thickness close to 15 cm revealed a time lag of about 6 h. The time lag measured for the brick containing hydrated salts is 2 h 40, that is almost 2.5 times shorter. This can be an inconvenient if the wall is devoted to be installed in an inhabited dwelling to take advantage of gains at the end of the day, but becomes an advantage for installation in premises occupied during the day such as school, offices or commercial buildings.

Another part of the study was devoted to evaluate the efficiency of the solar wall. It has been discussed that this efficiency could be improved in limiting losses to the outside and increasing exchanges in the cavity. The last part of the work was specifically devoted to the thermal study of the brick containing PCM. It showed, through measures of fluxes and temperatures, the specific thermal behavior of this kind of material. The melting phase of the PCM at 27 °C was observed as the storage phases of sensible energy. When the wall discharges energy during the night, the solidification phase accompanied by a sudden release of heat has been highlighted. The difference between the melting and solidification temperatures, related to the supercooling phenomenon was clearly showed during the day–night cycles.

The specific thermal behavior of a PCM, formed here of hydrated salts is complex to model especially in the solidification phase. In this study, the wall is composed of nine bricks because of their diverse positions, each brick reacts differently to solar radiation and heat transfers in the ventilated channel. The experimental data presented in this article will be necessary to validate it.

Acknowledgements

The authors are very grateful to the program ANR-PREBAT which financed the work and to Artois Comm and the Nord Pas de Calais Region for financing the Ph.D. thesis of Zohir Younsi.

References

Ahmad, M., Bontemps, A., Sallée, H., Quenard, D., 2006. Experimental investigation and computer simulation of thermal behaviour of wallboards containing a phase change material. Energy and Buildings 38 (4), 357–366.

Alzoubi, H., Alshboul, A., 2010. Low energy architecture and solar rights: restructuring urban regulations. View from Jordan original research article. Renewable Energy 35 (2), 333–342.

ASHRAE handbook, 1993, Fundamentals, ISBN: 0-910110-96-4.

Askew, G.L., 1978. Solar heating utilization a paraffin's phase change material. In: Proceedings of the second national passive solar conference, Philadelphia, PA.

Benard, C., Body, Y., Gobin, D., Guerrier, B., 1982. Use of a variable parameter test-cell for the study of latent-heat solar walls. Solar Energy 29 (2), 101–109.

Benard, C., Body, Y., Zanoli, A., 1985. Experimental comparison of latent and sensible heat thermal walls. Solar Energy 34 (6), 475–487.

Benson, D.K., Webb, J.D., Burrows, R.W., McFadden, J.D.O., Christensen, C., 1985. Materials research for passive solar systems: solid-state phase-change materials, Solar Energy Research Institute, US Department of Energy Contract EG-77-C-01-4042.

Bourdeau, L., 1980. Study of two passive solar systems containing phase change materials for thermal storage. In: Hayes, J., Snyder, R. (Eds.), Proceedings of the Fifth National Passive Solar Conference, 19–26 October, Amherst, Newark, DE, American Solar Energy Society, pp. 297–301.

Bourdeau, L., 1982. Utilisation d'un matériau à changement de phase dans un mur Trombe sans thermocirculation. Revue Phys Appl 17, 633–642.

Bourdeau, L., Jaffrin, A., 1979. Actual performance of a latent heat diode wall. In: Proceedings of Izmir International Symposium II on Solar Energy Fundamentals and applications, Izmir Turkey.

Bourdeau, L., Jaffrin, A., Moisan, A., 1980. Captage et stockage d'énergie solaire dans l'habitat par le moyen de mur diode à chaleur latente. Revue Phys Appl 15, 559–568.

Boutin, Y., Gosselin, L., 2009. Optimal mixed convection for maximal energy recovery with vertical porous channel (solar wall). Renewable Energy 34 (12), 2714–2721.

Christensen, C., 1983. Advanced Phase-Change Storage: Analysis of Materials and Configurations 8th National Passive Solar Conference, Santa Fe, NM, USA.

Cristopia website, <http://www.cristopia.com/indexCristopia.html>, (accessed 27.11.2010).

Diaconu, B., Cruceru, M., 2010. Novel concept of composite phase change material wall system for year-round thermal energy savings original research article. Energy and Buildings 42 (10), 1759–1772.

Eiamworawutthikul, C., Strohbehn, J., Harman, C., 2002. Investigation of phase change thermal storage in passive solar design for light-construction building in the southeastern climate region. A Research Program to Promote Energy Conservation and the Use of Renewable Energy, Pratt School of Engineering Duke University, <http://energy.pratt.duke.edu/document/Temporary/PDF_2.pdf>, (accessed 27.06.2011).

Farouk, B., Guceri, S.I., 1981. Trombe–Michel wall using phase change materials (for solar heating of buildings), Alternative energy sources II, In: Proceedings of the Second Miami International Conference, Miami Beach, Fla, United States, pp. 493–502.

Ghoneim, A.A., Klein, S.A., Duffie, J.A., 1991. Analysis of collector—storage building walls using phase change materials. Solar Energy 47 (1), 237–242.

Gratia, E., Deherdea, 2007. Are energy consumptions decreased with the addition of a double-skin. Energy and Buildings 39 (5), 605–619.

Jie, J., Hua, Y., Gang, P., Bin, J., Wei, H., 2007. Study of PV-Trombe wall assisted with DC fan. Building and Environment 42 (10), 3529–3539.

Khalifa, A.J.N., Abbas, E.F., 2009. A comparative performance study of some thermal storage materials used for solar space heating. Energy and Buildings 41, 407–415.

Knowles, T., 1983. Proportioning composites for efficient thermal storage walls. Solar Energy 31 (3), 319–326.

Leclercq, D., Thery, P., 1983. Apparatus for simultaneous temperature and heat flux measurements under transient conditions. Review of Scientific Instruments, 54.

Manz, H., Egolf, P.W., Suter, P., Goetzberger, A., 1997. TIM–PCM external wall system for solar space heating and daylighting. Solar Energy 61 (6), 369–379.

Onishi, J., Soeda, H., Mizuno, M., 2001. Numerical study on a low energy architecture based upon distributed heat storage system. Renewable Energy 22, 61–66.

Sandnes, B., Rekstad, J., 2006. Supercooling salt hydrates: stored enthalpy as a function of temperature. Solar Energy 80 (5), 616–625.

Shen, J., Lassue, S., Zalewski, L., Huang, D., 2007. Numerical study on thermal behaviour of classical or composite Trombe solar walls. Energy and Buildings 39 (8), 962–974.

Şişbot, S., 2005. A cross-correlation technique as a system evaluation tool; application to blood flow measurement in extra-corporeal circuits. Flow Measurement and Instrumentation 16 (1), 27–34.

Stritih, U., Novak, P., 1996. Solar heat storage wall for building ventilation. Renewable Energy 8 (1–4), 268–271.

Swet, C.J., 1980. Phase change storage in passive solar architecture. In: Proceedings of the Fifth National Passive Solar Conference, Amherst, MA, pp. 282–286.

Takamoto, M., Ishikawa, H., Shimizu, K., Monji, H., Matsui, G., 2001. New measurement method for very low liquid flow rates using ultrasound. Flow Measurement and Instrumentation 12, 267–273.

Telkes, M., 1978. Trombe wall with phase change storage material. In: Proceedings of the 2nd National Passive Solar Conference, Philadelphia, PA, USA.

Telkes, M., 1980. Thermal energy storage in salt hydrates. Solar Energy Materials 2, 381–393.

Tiwari, G.N., Yadav, Y.P., Lawrence, S.A., 1988. Performance of a solarium: an analytical study. Building and Environment 23 (2), 145–151.

Wild, J.A., Moses, P.J., Strom, E.E., 1985. Performance measurements of a phase-change Trombe wall in a calibrated hot box and unoccupied test houses, 91:2B; Conference: American Society of Heating, Refrigerating and Air-Conditioning Engineers' semiannual meeting, Honolulu, HI, USA.

Yinping, Z., Guobing, Z., Kunping, L., Qunli, Z., Hongfa, D., 2007. Application of latent heat thermal energy storage in buildings: state-of-the-art and outlook. Building and Environment 42 (6), 2197–2209.

Younsi, Z., Lassue, S., Zalewski, L., Joulin, A., 2007. Thermophysical characterization of phase change materials for the storage of solar energy in building. In: International Conference on Heat Transfer in Components and Systems for Sustainable Energy Technologies Heat-SET 2007, Chambery, France.

Younsi, Z., Zalewski, L., Rousse, D., Joulin, A., Lassue, S., 2008. Thermophysical characterization of phase change materials with heat flux sensors. In: Proceedings of Eurotherm, 5th European Thermal-Sciences Conference, Eindhoven, the Netherlands, ISBN 978-90-386-1274-4.

Zalba, B., Marín, JM., Cabeza, LF., Mehling, H., 2003. Review on thermal energy storage with phase change: materials, heat transfer analysis and applications. Applied Thermal Engineering 23 (3), 251–283.

Zalewski, L., Chantant, M., Lassue, S., Duthoit, B., 1997. Experimental thermal study of a solar wall of composite type. In: Energy and Buildings, vol. 55. Elsevier Science, pp. 8–17.

Zalewski, L., Lassue, S., Duthoit, B., Butez, M., 2002. Study of solar wall – validating a simulation model. Building and Environment (Pergamon) 37, 109–121.

Zrikem, Z., Bilgen, E., 1987. Theoretical study of a composite Trombe–Michel wall solar collector system. Solar Energy 39 (5), 409–419.

Zrikem, Z., Bilgen, E., 1989. Annual correlations for thermal design of the composite wall solar collectors in cold climates. Solar Energy 42 (6), 427–432.